Filmogen Organic–Inorganic Hybrids Obtained by Sol–Gel in the Presence of Cationic Polymer

Dan Donescu,[1] Sever Serban,[1] Violeta Uricanu,[2] Michel Duits,[2] Alain Perichaud,[3] Mihaela Olteanu,[4] Manuela Spiroiu,[4] Marilena Vasilescu[5]

[1]*Institute of Chemical Research, Splaiul Independentei 202, 77208, Bucharest, Romania*
[2]*Applied Physics Department/NCV, University of Twente, Postbus 217, 7500 AE Enschede, Netherlands*
[3]*Laboratoire de Chimie Macromoléculaire, UMR-CNRS 6171, Service 461, Université Paul Cézanne, Avenue Normandie-Niémen, 13397 Marseille Cedex 20, France*
[4]*Physical Chemistry Department, University of Bucharest, 70346, Bucharest, Romania*
[5]*Physical Chemistry Institute of the Romanian Academy, Splaiul Independentei 202, 77208, Bucharest, Romania*

Received 27 November 2006; accepted 9 April 2007
DOI 10.1002/app.26804
Published online 30 July 2007 in Wiley InterScience (www.interscience.wiley.com).

ABSTRACT: Self-standing and coated-on-glass films were prepared from polymer–inorganic ormosils, using the cationic polymer poly(methacrylamide propyl quaternarydimethyldodecyl bromide). The inorganic compound was grown in sol–gel reactions based on methyltriethoxysilane (MeTES), with or without addition of the titanium-precursor: tetraisopropyl orthotitanate. As evidenced by thermogravimetric analysis and differential scanning calorimetry data, the thermal properties of the films are highly dependent on the internal morphology. Inorganic granules with a TiO_2 rich shell have a more polar surface, which stimulates stronger electrostatic interactions with the polymer, hence, a reduced mobility for the amino end and a smaller probability to have amino ends engaged in interactions at the surface of the granules. Coated-on-glass films drawn from pure cationic polymer suffer from partial dewetting. Topographic and force-versus-distance recordings using atomic force microscopy showed a change in the energy balance and no dewetting regions were encountered for polymer/MeTES based composites. However, because of nongrafted polymer, these films are not immune at washing with water/acetone. Explorations of antibacterial activity against the gram-negative bacteria, *Pseudomonas aeruginosa*, were done using ormosil films with alkoxysilanes combinations. J Appl Polym Sci 106: 2625–2633, 2007

Key words: morphology; microstructure; inorganic materials; atomic force microscopy (AFM); thermal properties

INTRODUCTION

The efforts of the last years to obtain filmogen polymer–inorganic hybrids are justified by the need to improve the performances of usual polymers.[1–17] For filmogen[18,19] or nonfilmogen hybrids, dispersing nanometric-sized inorganics into polymer matrices, (i) an increase in both thermal and dimensional stabilities, (ii) improved physico-mechanical performances,[2–4,7,9] (iii) fire resistance,[9] (iv) decreased water absorption,[3] or (v) gas permeability[7,10] were achieved. Depending on the properties of the end-product, filmogen hybrids can be further used as waveguide materials with either nonlinear[1] or photochromic[11] properties, conducting films[6] membranes,[7,10] contact lenses,[15] and anticorrosive coatings.[16]

In what concerns the special case of cationic polymers, they are interesting candidates for organic–inorganic preparations since electrostatic interactions can strengthen the links between the reaction partners. Moreover, several cationic polymers were shown to have antibacterial activity.[20,21]

In the present paper we report our investigations on polymer–inorganic ormosils prepared with a newly synthesized cationic polymer, namely poly (methacrylamide propyl quaternarydimethyldodecyl bromide), abbreviated in the following text as PC_3.

As in our previous works,[22,23] we used different alkoxysilanes, with or without the addition of a titanium-compound.

EXPERIMENTAL

Materials

The alkoxysilanes, methyltriethoxysilane (MeTES), phenyltriethoxysilane (PTES), octyltriethoxysilane (OTES), and vinyltriethoxysilane (VTES), all products from Merck Schuchard, tetraisopropyl orthotitanate (TIP), (3-glycidoxypropyl) trimethoxysilane (GMPS), and 3(trimethoxysilyl)propylmethacrylate (MPTS) from FlukaAG and rhodamine B (A.R.) were used without further purification. Dimethyl aminopropyl methacrylamide, dodecylbromide, and 2,6-ditert-butyl-4-methylphenol (all from Catalyze, France) and

Correspondence to: V. Uricanu (violeta.uricanu@k.ro).

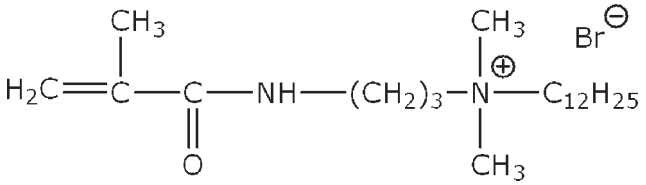

Figure 1 Chemical formula of the monomer.

glycerol, ethylene glycol, α-bromnaphtalene, chloroform, and 2,2-azoisobutyronitrile (AIBN) (all Sigma products) were used as received. Ethanol (Chimopar, Romania) was purified by rectification. Maleic anhydride (MA) (Reagent) was purified by sublimation.

Polymer

The monomer (3-methacrylaminopropyl)-*N*,*N*-dimethyl-1-dodecylammonium bromide (see Fig. 1) was obtained by quaternisation of dimethyl aminopropyl methacrylamide with dodecylbromide in ethanol, at 80°C for 10 h. 2,6-Ditert-butyl-4-methylphenol (800 ppm) was added as inhibitor against polymerization. In the next step, the quaternized monomer was purified by precipitation in chloroform. Further, the monomer was resolubilized in ethanol and polymerized using AIBN, under nitrogen, at 80°C for 3 h. The final polymer, recovered after precipitation with nonsolvent, was resolubilized and characterized using light scattering. An average molar mass of $(50 \pm 0.05) \times 10^3$ g/mol was found.

Film preparation

In all ormosil–polymer recipes, the cationic polymer was dissolved in 8 mL ethanol prior to the addition of the other reagents for the sol–gel reaction. A constant amount of methyl-containing precursor (i.e., 2.25 g MeTES) was used. Meanwhile, the amount of cationic polymer was changed (see Table I). The inorganic precursor MeTES was hydrolyzed for 4 h with acidic water (0.44 g, 0.01*M* HCl), under continuous stirring.

In compositions with TIP, MA was used as a complexing agent that slows down the sol–gel process of the titanium compound.[24] When TIP was incorporated in the recipe, the hybrids were prepared by a two-step method because TIP hydrolyzes at a much higher rate than MeTES.[25,26] After a prehydrolysis step with 0.14 g acidic water for 2 h, the TIP and maleic anhydride were added to the solution, together with the second portion of water (0.3 g). The mixture was stirred for another 2 h.

In addition, composites with PC3 (0.8 g), TIP (0.2 g), and variable MeTES/RTES combinations were prepared also via the two-step method. These films can be identified by the index: PC_3-Me-R-TIP, with R denoting the organic moiety attached to the silanes precursor. This moiety was changed from methyl (MeTES) to: phenyl (PTES), octyl (OTES), propylmethacrylate (MPTS), vinyl (VTES), or 3-glycidyloxypropyl (GMPS). In the recipes with combinations of silica-precursors, the initial amount of MeTES (2.25 g) was replaced with an equal amount of a 1 : 1 mixture of MeTES : RTES.

All final sols were homogeneous and fluid. For AFM and wettability investigations, thin films were deposited on glass slides (precleaned with piranha solution, repeatedly washed with water, EtOH, and dried under nitrogen) by dip-coating. The slides were left further to dry at room temperature (25°C), under a mild nitrogen stream, for 2 weeks. No macroscopic cracks (i.e., visible with eye resolution) were observed after drying. The thickness of the films, the profile, and the extent of thickness variation along the film surface were measured with a profilometer (Talystep Taylor Hobson). All the final films had a thickness of ≈ 30 μm. For the thermogravimetric analysis (TGA) analysis, well-determined amounts from all formulations were deposited on poly(ethylene) sheets and dried in similar conditions (as the other samples). Before measurements, the

TABLE I
Films Indices and Appearance

Film index	Polymer/silane (%)	Polymer (g)	TIP/MA (g/g)	Appearance of the film	
				Transparency	Strength
PC0-Me	0	–	–	Opalescent	Flexible, soft
PC1-Me	8.2	0.2	–	Opalescent	Flexible, soft
PC2-Me	15.2	0.4	–	Opalescent	Flexible, soft
PC3-Me	26.2	0.8	–	Transparent	Flexible, soft
PC0-Me-TIP	0	–		Opalescent	Flexible, hard
PC1-Me-TIP	8.2	0.2	0.2 / 0.038	Opalescent	Flexible, hard
PC2-Me-TIP	15.2	0.4		Opalescent	Flexible, hard
PC3-Me-TIP	26.2	0.8		Transparent	Flexible, hard
PC3	100	0.8	–	Transparent	Brittle
PC3-TIP	26.2	0.8	0.2 / 0.038	Transparent	Flexible, hard

In all recipes with MeTES, 2.25 g were used.

polymer substrate was peeled off, yielding self-standing composite films.

Methods

TGA was carried out at a heating rate of 20°C/min in air using a Du Pont 2000 instrument. Same instrument was used for differential scanning calorimetry (DSC), at a speed of 10°C/min. To avoid artefacts in the DSC curves, the recordings presented in this paper were made after an initial heating (up to 120°C)–cooling cycle.

Wettability studies were conducted according to the liquid–solid contact angle method. A tiny drop (from a liquid with known properties) is gently deposited on the solid surface of the film and the contact angle is measured during a time interval of several seconds. The image of the drop profile is recorded by video enhanced microscopy. Using the same procedure, the contact angles were measured using four different liquids: water, glycerol, ethylene glycol, and α-bromnaphtalene. On the basis of the obtained values, the Lifshitz-van der Waals (γ_L^{LW}) and acid–base (γ_L^+ and γ_L^-) contributions of the surface tensions were calculated as in ref. 23.

A home-built instrument (Twente University, The Netherlands) was used to observe the structure (height profile) at the film/air interface. The microscope was operated in constant force imaging mode at a setpoint control force of 5 nN in air. Also, the interaction between the AFM tip of the cantilever and the films was measured in air with the instrument operated in the force-versus-distance mode. The silicon nitride cantilever (Park Scientific Instruments, with a nominal spring constant 0.1 N/m) was driven up and down at a frequency of 1 Hz. Contact mode AFM and force-versus-distance scans were performed on the film surface as obtained after drying and, also, on ''washed'' films. The latter ones were obtained by flushing the films' surface at room temperature with water (2 min), followed by acetone (2 min), and finally redrying at room temperature.

Fluorescence emission spectra were recorded with a Perkin Elmer 204 spectrophotometer equipped with a 150 W xenon lamp as the excitation source ($\lambda_{excitation}$ = 360 nm).

The testing of the antibacterial activity was done using the gram-negative bacteria, *Pseudomonas aeruginosa*, prepared as suspension in peptonated water at a concentration of 5×10^6 cells per mL. For these tests, the composite films were first deposited on filter paper pads (10×20 mm^2). Experiments with clean pads were done as ''witness.'' A standard method for antibiotics tests was used, following the protocol below. The pads were first carefully put on top of culturing media (blood gelose) supported in Petri dishes with diameters larger than the surface of the pads. Next, 0.3 mL of bacteria suspension was pipetted on top of the free culturing medium, the so-conditioned specimens were incubated for 24 h at 37°C, afterwards kept at ambient temperature and examined every day.

RESULTS AND DISCUSSIONS

In our earlier work,[23] using different RTES precursors, we found that polymer-free composites with MeTES and TIP have a very regular structure (made from spherical granules with a diameter around 46 nm) and a high resistance against washing with solvent. Because of the special composition, i.e., a compact silica-rich core surrounded by a more porous shell with a predominant TiO_2 composition, dye incorporation and retention are exceptionally good. As evidenced by transmission electron microscopy,[23] for preparations made only with MeTES, the porous shell does not exist and washing with water/acetone induces a small removal of dye.

The main difference between the ormosils prepared in Ref. 23 and the composites, which are the focus of this report, is the presence of an added polymer, which is not grafted to the inorganic structures, but has the capability to interact with them, especially at the end of the formulation, after stirring is stopped and the sols are deposited for solvent evaporation.

The films casted from the MeTES and MeTES-TIP composites have been first analyzed with FTIR. For the pure PC_3-polymer, one can distinguish the following peaks in the FTIR spectra [Fig. 2(a,b)]:

- at 1650 cm^{-1}, a strong stretching vibration of the C=C group conjugated with C=O;
- at 1530 cm^{-1}, also a strong peak attributed to the amine moiety O=C—N—, which is H-bonded and in the *trans* configuration;
- the twin peaks at 1490 and 1465 cm^{-1} represent the symmetric and asymmetric C—H deformation vibrations from the CH_3 groups linked to the quaternary ammonium N^+;
- the contributions at 1200 and 970 cm^{-1} are the C—N stretching vibrations (due to the amine arrangement of the first N);
- in the region 670 cm^{-1} down to 400 cm^{-1}, there is a superposition of two contributions, which are the skeletal vibrations of the alkene group.

Using MeTES in preparations, additional peaks indicate the formation of an inorganic compound with the Si—O—Si strong contribution dominating in the 1000–1150 cm^{-1} spectral region [Fig. 2(a)]. The Si—O—Si symetric stretching gives a contribution at $\sim$ 770 cm^{-1}. The presence of a peak at 1270 cm^{-1},

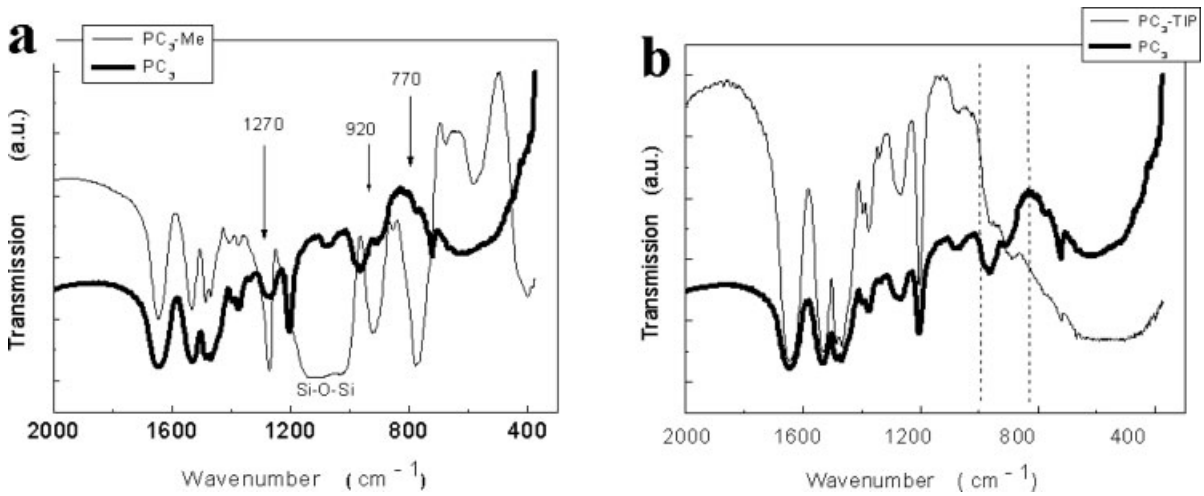

Figure 2 FTIR spectra for films prepared from cationic polymer (PC_3) added to the sol–gel recipe with MeTES (a) or TIP (b).

specific to C—O bending in Si—O—C, is an indication that the inorganic compound is not fully hydrolyzed and the composite film contains a fraction of ethoxy groups attached to the inorganic network.

The individual contributions from the skeletal alkene groups are more easy to identify in the films PC_i-Me (with $i = 1$, 2 or 3), e.g., see Figure 2(a), the peaks at 680, 590, and 405 cm^{-1} for PC_3-Me.

For the hybrids PC_i-Me-TIP, the FTIR spectra were found to be identical with PC_i-Me, since the small contribution expected at $\sim$ 960 cm^{-1} for Si—O—Ti groups is screened by the strong silica contribution. By contrast, in PC_3-TIP, the presence of the Ti—O—Ti links changes the shape of the spectra in the 1000–850 cm^{-1} range [see the region between the dotted lines in Fig. 2(b)].

Thermal properties

TGA measurements provide information about the thermal stability and reflect the bulk properties of the end materials produced via the sol–gel method. The pure polymer has two main degradation steps, with significant weight losses at temperatures around 244°C (oxidative degradation) and 320°C (scission of the main chain) [Fig. 3(a,b)].

A noticeable increase in the thermal stability of the cationic polymer was found for all polymer–inorganic hybrids with MeTES [Fig. 3(a,c)]. Using DTG curves [like Fig. 3(b)], a specific identification of the individual (i.e., per degradation step) maximum rates for thermal decompositions proves that the inorganic reduces the contact of polymer's vulnerable organic moieties with the oxygen. These results are in good agreement with previously published data.[6,9,22,27]

A visible shift towards lower temperatures for the oxidative step is seen for the TiO_2 containing films [Fig. 3(c) compared with Fig. 3(a)]. This decrease goes so far that, for the hybrid PC_3-TIP, the end-product is even more susceptible to thermal decomposition than the starting pure polymer [see Fig. 3(d) compared with Fig. 3(b)]. The observed effect can have two sources. The first one is a modified morphology of the granules (as demonstrated in Ref. 23 for Me-TIP granules when compared with particle made from pure MeTES) and, hence, a different interaction of the organic chains with the inorganic matrix. The second explanation can be a catalytic effect of TiO_2 on the thermal oxidation.[28]

TIP presence in the initial recipes also stimulates an advanced thermal degradation at temperatures above 400°C [Fig. 3(d)].

Polymer contacts with the inorganic are sensitive to the local polarity and specific interactions. Differences in the chain mobility would be expressed in differences in the temperatures associated with conformational transitions. These can be measured with DSC.[29–31] The endothermic peak (around 110°C) in the DSC curve of the pure polymer indicates that, in bulk, the cationic polymer has a certain degree of association induced by the dipolar interactions at the amine groups (for which FTIR showed hydrogen bonding). At higher temperatures, thermal degradation begins and gives in the DSC curve an exothermic signal.

When the starting material is a mixture between polymer and the sol–gel result of MeTES hydrolysis, few additional features are visible. The endothermic peak has two contributions: one being identical with the pure (bulk) polymer and a second contribution at lower temperatures (denoted II in Fig. 4). Then, there is another endothermic transition in the tem-

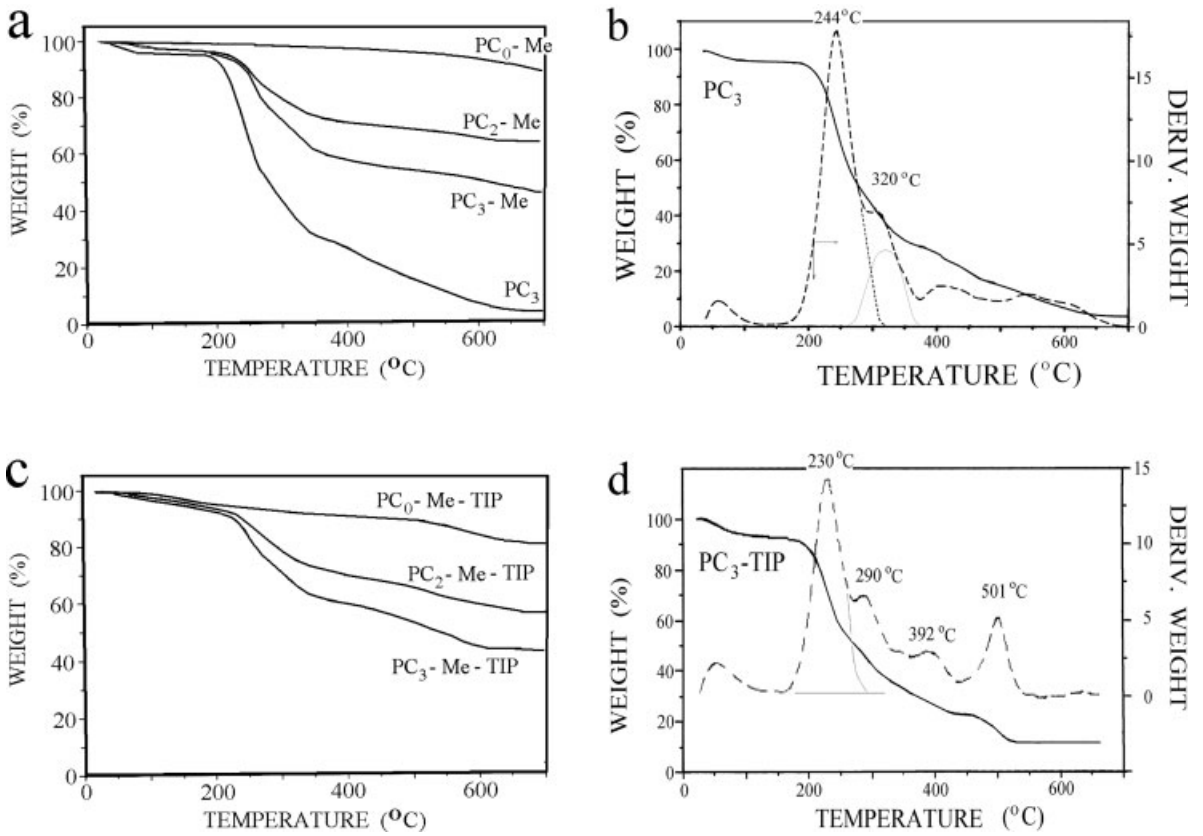

Figure 3 Thermogravimetrical curves (full lines) and derivative DTG curves (dotted lines) for several hybrids.

perature range 180–230°C (marked III, Fig. 4), followed by thermal degradation.

If the composite is prepared with both silica and titania precursors, the II-nd and III-rd contributions are much closer to the polymer main peak (I). On the hybrid PC_3-TIP, the DSC curve has only the I and III-rd contribution, with the last one around 125°C.

We can ask ourselves: how can these observations be reconciliated in a generic picture?

The answer is related with the possible interactions inside the composite materials. One should recall that the cationic character of the polymer would stimulate electrostatic interactions with negative sites on the inorganic. If these interactions are weak, the amine end of the polymer has enough mobility to search for favorable orientations and find its interaction companions (i.e., other amine groups from neighboring chains). Taken into account that the resulting bridges are in a constrained configuration, like a network very close to the silica surface, dipol–dipol interactions with the inorganic may strengthen even more these superficial orderings, hence generating configurations less susceptible to temperature. The melting peak at temperatures higher than those measured for pure, bulk PC (i.e., the III-rd peak) supports this hypothesis. On the

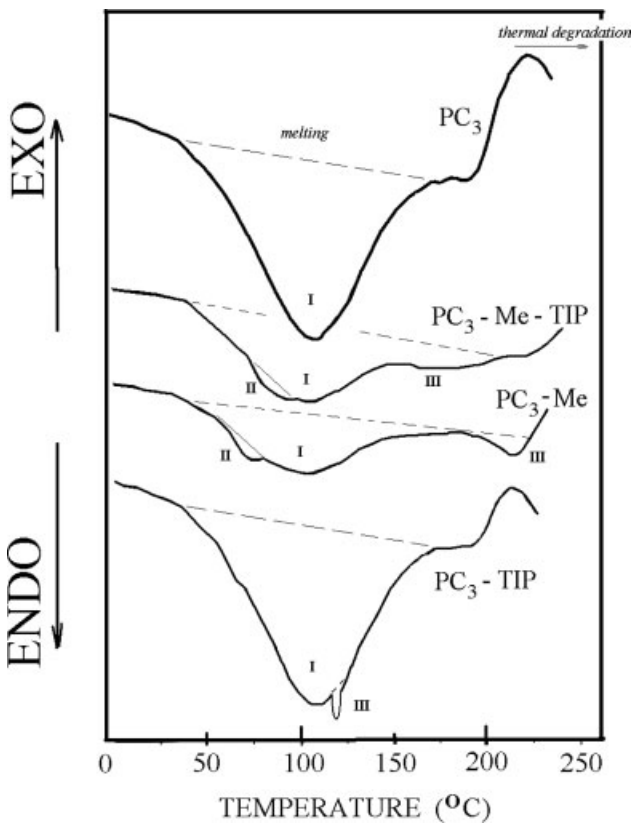

Figure 4 DSC thermograms of various hybrids.

other hand, because of these ''surface-tight'' arrangements, the Br-terminated alchilic end will be forced to form a sort of polymeric brush, with a small degree of ordering, expressed in the appearance of peak II.

For formulations with MeTES and TIP, if the resulting granules have a TiO_2 rich shell, the surface will have a higher superficial polarity and a higher affinity for interactions. In these conditions one can expect stronger electrostatic interactions, which means a reduced mobility for the attached amino end and a smaller probability to have amino ends engaged in interactions at the surface of the granules. This is the reason why peak III is almost ''embedded'' at the end of peak I for the composite PC_3-Me-TIP and peak II has almost disappeared. In the film made from PC_3-TIP, peak III remains slightly more visible than in PC_3-Me-TIP.

Differences in polarities at the microscopic level can also be evidenced if a dye is used as ''marker.'' According to the recipe already used in ref. 23, rhodamine B was added as ethanolic solution at the end of the sol–gel process, stirred for another 2 h before casting films from the end products. After drying, the films have been subjected to fluorescence spectroscopy, with identification of the emission maxima. For pure PC_3 and films in the series: PC_i-Me, (with i = 1–3) the same value was obtained: 564 nm. In contrast, the dye-doped formulation prepared only with MeTES had the maximum at 557.5 nm. Such a red shift in the position of the emission maximum indicates a higher polarity in the microvicinity of Rh-B in the hybrids when compared with pure inorganic. The red shift is even bigger for the film series: PC_i-Me-TIP (with i = 0–3), in perfect agreement with a higher polarity due to the TiO_2. If we compare the obtained value, 570 nm, with the one obtained on TiO_2/SiO_2 hybrids in ref. 23 (namely 578 nm), the data suggest that polymer interactions with the polar sites on the TiO_2-rich shell of the granules creates a less polar microenvironment.

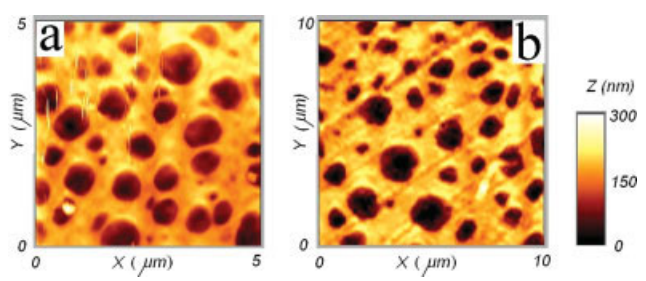

Figure 5 Topography of the PC_3 film, from pure polymer, as prepared (left image) and after washing (right image). Please note the two different length scales on the images: 5 μm, left and 10 μm, right. [Color figure can be viewed in the online issue, which is available at www.interscience.wiley.com.]

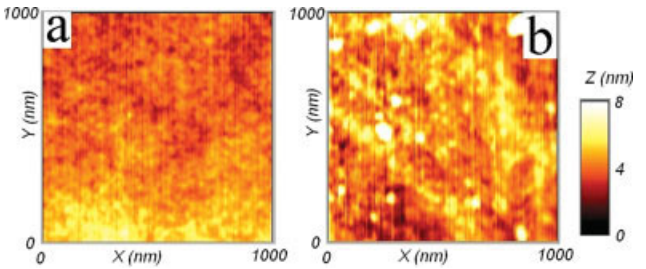

Figure 6 Topography of a sol–gel PC_0–Me film, as prepared (a) and after washing (b). [Color figure can be viewed in the online issue, which is available at www.interscience.wiley.com.]

Characterization of the film surface: wettability and AFM data

Continuing with the investigations at the nanoscale, nondoped films obtained by coating-on-glass have been used for topographical imaging, using AFM (contact mode). The film cast from pure polymer is not flat, but has irregular small holes, which are formed during solvent removal after film deposition on glass. Such a partial dewetting was seen also for other combinations polymer–substrate and is attributed to instabilities generated by the interplay between the energy in the film and the interaction with the surface. (For more details the reader can see ref. 32 and references therein.) If the surface is washed, the holes grow in size (i.e., the surface imaged in Fig. 5—right is actually four times bigger than the image on the left).

For a film drawn from PC_0-Me (i.e., with no polymer), the topography resembles the morphology also found in ref. 23: small granules of inorganic material can be easily identified in Figure 6(a). Washing the surface of the PC_0-Me film with water and acetone stimulates a reorganization of the granules located in the superficial layers and few particle–aggregates are visible in Figure 6(b).

Using different amounts of polymer in the hybrid formulations also generates less regularity at the film surfaces. An example of it is given in Figure 7(a),

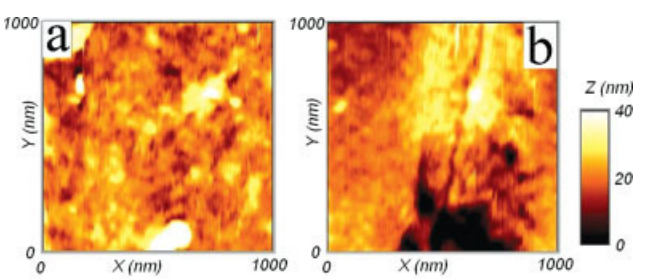

Figure 7 As prepared (a) and washed (b) surface for a film made with the hybrid PC_3-Me, imaged with AFM. [Color figure can be viewed in the online issue, which is available at www.interscience.wiley.com.]

which shows that the very regular granules seen for PC_0-Me [Fig. 6(a)] are now replaced in PC_i-Me with aggregates of various sizes. The formation of these agglomerations has its source in the electrostatic polymer–inorganic interactions (as explained already in the text).

Since no grafting agent (for the polymer chains in the film) was used, the polymer is easily removed by washing and the remaining surface [see Fig. 7(b)] shows characteristics seen already: regular granules in the inorganic regions [like in Fig. 6(a)] and empty regions (or holes), like in Figure 5(a,b). The most noticeable influence of the inorganic on the general aspect of the hybrids is the holes' disappearance in the initial (unwashed) films. The presence of the inorganic and its interactions with the cationic organic chains changes the energy balance and no dewetting regions are encountered for PC_i-Me composites. However, because of nongrafted polymer, these films are not immune on washing.

Similar observations, as obtained with AFM for PC_i-Me films, also hold for the PC_i-Me-TIP composites.

The AFM silicone nitride tip is polar and, in the force histograms obtained from force-versus-distance measurements, the polar–polar interactions are reflected in higher adhesion forces when compared with (tip) polar–nonpolar (sample) interactions.

A relative high incidence of the CH_3-groups covering the inorganic spheres in PC_0-Me gives a narrow force histogram (not shown here), with adhesion forces between 2 and 4 nN. On the contrary, for the pure polymer film, enhanced interactions between the cationic ends of the polymer and the negatively charged AFM tip shift the force histogram to higher forces: 12–14 nN. In the organic–inorganic hybrids, PC_i-Me, it seems that only a part of the charged ends of the cationic polymer are facing the inorganic and the adhesion values are spread between 4 and 8 nN. In the PC_3-TIP hybrid, the polymer contribution dominates.

Two populations, with different polarities, contribute to the force histogram for washed PC_i-Me. While the first population has characteristics similar to the as prepared films (i.e., adhesion = 4–8 nN), the second population belongs to pure polymer islands (more polar: 12–14 nN), which have been created after partial mobilization of the polymer by the solvent combination used in the washing step.

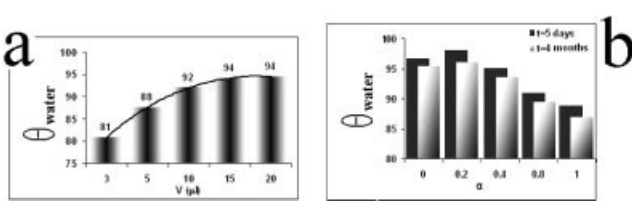

Figure 8 (a) Equilibrium contact angle as a function of the volume of the deposited water drop. Example given for a PC_1-Me film. (b) Influence of the polymer-to-inorganic ratio (expressed here via the coefficient α which is equal with the polymer amount in the PC_i-Me; α = 1 denotes PC_3).

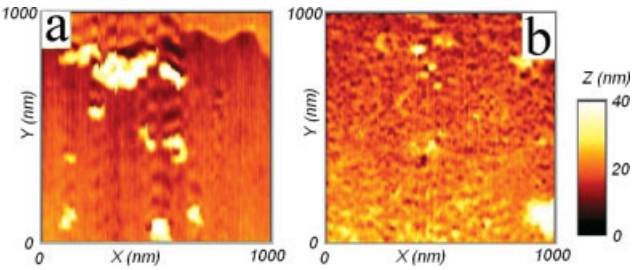

Figure 9 AFM imaging of the film surface before (a) and after (b) washings with water/acetone, for the hybrid PC_3-Me-GMPS-TIP. [Color figure can be viewed in the online issue, which is available at www.interscience.wiley.com.]

Polymer solubility in water also affects the measurement of the contact angles. (These measurements were part of the wettability studies, which give an average over the film superficial properties at the macroscale.)

A variation of the contact angle with water [like in Fig. 8(a)] was seen for small drops deposited on all films with polymer. For drop volumes larger than 15 µL, an equilibrium value is attained. The composition of the hybrids has detectable influence on the hydrophilic–hydrophobic balance at the surface. As expected, with the addition of more polymer [i.e., increase of the α index in Fig. 8(b)], the hybrids are more hydrophilic. Kept in the dried state, the films proved to be quite stable and no significant variations in the contact angles were seen between measurements done after 5 days or 4 months from films' deposition. The presence of TIP in the PC_i-Me-TIP hybrids was not noticed in the wettability studies and identical data were obtained as for PC_i-Me.

Hybrids with alkoxysilanes combinations (PC_3-Me-R-TIP)

Using combinations of alkoxysilanes, the properties of the hybrids can be more finely tuned towards desired directions (see examples below).

A better coverage of the granular inorganic with organic material [see Fig. 9(a) compared with Fig. 7(a)] and smaller degree of agglomeration after washing [Fig. 9(b) compared with Fig. 6(b)] was obtained for PC_3-Me-GMPS-TIP. This composite also has the highest internal polarity (Fig. 10).

The differences in the internal polarity were investigated using rhodamine (Rh-B) as marker (see Fig. 10). The measured emission band of Rh-B results from electronic transitions, which are changes from

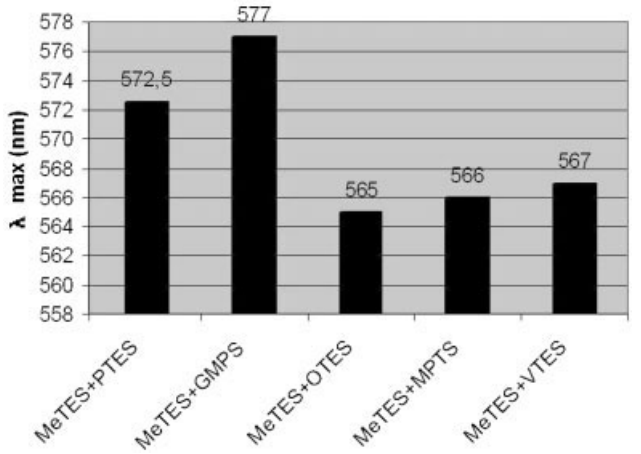

Figure 10 Changes of the wavelength of the emission peak (λ_{max}) for fluorescence spectra of rhodamine B-doped hybrids, as a function of composition. All hybrids belong to the PC_3-Me-R-TIP series.

the vibrationally lowest-lying level of the first excited electronic state S_1 to the vibrationally excited sublevels of the electronic ground state.[33]

The wavelength (around 580 nm) of the peak characteristic for the fluorescence emission spectra of the dye-doped hybrids confirm that Rh-B exists in the cationic form in these composites.[34,35] Blue shift of the peak positions (from 580 nm towards 560 nm) are an indication for the decrease in Rh-B cationic species and formation of new species at the expense of this cation. In dye-doped solids, highly acidic cage environment is capable to supply more protons (H^+) to rhodamine-B cation. These (H^+) ions are attached to the nitrogen atom (uncharged) carrying a lone pair of electron in the structure of Rh-B cation, resulting higher protonated form. Because of Coulombic repulsive interactions, the attachment of H^+ ion at the nitrogen atom carrying positive charge is not possible. Thus, a higher protonated form of Rh-B induces a blue shift in the fluorescence peak of the dye in the hybrid films. The balance between the cationic form and higher protonated forms of Rh-B is the basis for the different λ_{max} values obtained for the fluorescence peaks of the composites (Fig. 10). Besides a high internal polarity, PC_3-Me-GMPS-TIP also has the best antibacterial activity (see Table II).

TABLE II
The Bacteria's Penetration Index (BP) Through the Sample Indicates a slight (BP = 1) or Complete (BP = 2) Damage Caused by the Microorganisms

Hybrid	Incubation time			
	24 h	48 h	72 h	144 h
Witness (paper support only)	2	2	2	2
PC0-Me-TIP	0	0	1	2
PC3-Me-TIP	0	1	1	2
PC3-Me-PTES-TIP	0	1	1	2
PC3-Me-GMPS-TIP	0	0	0	0
PC3-Me-OTES-TIP	0	0	0	0
PC3-Me-MPTS-TIP	2	2	2	2

For samples with 100% antibacterial activity: BP = 0 (no penetration).

TABLE III
The Surface Energy (mJ/m^2) Components of Hybrid Films with RTES

Hybrid film	γ_S^{LW}	γ_S^+	γ_S^-	γ_S^{TOT}
PC3-Me-TIP	39.058	0.006	0.109	39.078
PC3-Me-PTES-TIP	37.220	0.041	1.916	37.650
PC3-Me-GMPS-TIP	35.806	0.023	1.637	36.067
PC3-Me-OTES-TIP	31.068	0.017	0.096	31.134
PC3-Me-MPTS-TIP	36.412	0.025	1.721	36.618
PC3	39.149	0.696	4.321	39.271

The Lifshitz-van der Waals (γ_S^{LW}) surface energy is related with the interaction between the film components as manifested at the solid/air interface. Meanwhile, the acid-base (γ_S^+ and γ_S^-) contributions indicate the surface character as electron acceptor or, respective, donor.

The pads treated with PC_3-Me-GMPS-TIP, as well as the ones with PC_3-Me-OTES-TIP, are well protected against bacterial attack and no bacterial growth was seen on the pads, around, or under the pads. In all other cases, the bacteria spread around and under the pads (Table II).

For the time being one can only advance a hypothetical explanation for the antibacterial activity of some of the composites. The materials having advanced biocidal capabilities (i.e., PC_3-Me-GMPS-TIP and PC_3-Me-OTES-TIP) do not share identical values for surface (Table III) or internal (Fig. 10) polarities. However, these composites have the longest alkylic chains. The presence of a long alkylic chain was already proved to have antibacterial effects[21] for the PC_3 alone.

For long-term stability and resistance against solvents, it is recommended to have a grafting of the polymerizable chains in the hybrids, after film deposition. This can be achieved using an UV-activated initiator (as in ref. 22). We expect that antibacterial activity will be maintained in the grafted state, as it was seen already for polyamide fibers grafted with methacryloyloxyethyl dimethyldodecylammonium bromide.[21]

CONCLUSION

Different properties of film casted from complex combinations of the cationic polymer poly(methacrylamide propyl quaternarydimethyldodecyl bromide) with sol–gel structures obtained from Si-based alkoxysilanes, with or without TIP, were investigated. Our findings can be used for fine-tuning the preparation recipe for dedicated end-products.

The most important finding is the possibility to obtain coated-on-glass films without discontinuities (i.e. dewetting holes) for polymer/MeTES based composites.

Even if the here-presented studies of antibacterial activity are still far from being complete, they are a promising beginning along the path of certifying coatings immune to bacterial attack.

References

1. Prasad, P. N.; Bright, F. V.; Narang, U.; Wang, R.; Dunbar, R. A.; Jordan, J. D.; Ivisshi, R. In Hybrid Organic–Inorganic Composites; Mark, J. E.; Lee, C. Y. C.; Bianconi, P. A., Eds.; American Chemical Society: Washington, DC, 1995; p 317. ACS Symposium Series v.585.
2. Chen, J. P.; Ahmad, Z.; Wang, S.; Mark, J. E.; Arnold, F. E. In Hybrid Organic–Inorganic Composites; Mark, J. E.; Lee, C. Y. C.; Bianconi, P. A., Eds.; American Chemical Society: Washington, DC, 1995; p 295. ACS Symposium Series v.585.
3. Ahmad, Z.; Wang, S.; Mark, J. E. In Hybrid Organic–Inorganic Composites; Mark, J. E.; Lee, C. Y. C.; Bianconi, P. A., Eds.; American Chemical Society: Washington, DC, 1995; p 291. ACS Symposium Series v.585.
4. Nguyen, Y. N.; Perrin, F. X.; Vernet, J. L. In Organic–Inorganic Hybrid Materials; Sanchez, C.; Laine, R. M.; Yang, S.; Brinker, C. J., Eds.; Materials Research Society: Warrendde, 2002; p 149. MRS Symposium Proceedings v.726.
5. Torres-Requena, A. F.; Acosta-Najarro, D. R. In Emerging Fields in Sol–Gel Science and Technology; Lopez, T. M., Avnir, D., Aegerter, M., Eds.; Kluwer Academic: New York, 2003; p 322.
6. Jang, S. H.; Han, M. G.; Im, S. S. Synth Mat 2000, 110, 17.
7. Hu, Q.; Marand, E. Polymer 1999, 40, 4833.
8. Hasegawa, K.; Tatsumisago, M.; Minami, T. J Ceram Soc Jpn 1997, 105, 569.
9. Narita, T.; Kikuchi, N.; Kawasaki, K.; Ozaki, Y. J Ceram Soc Jpn 1996, 104, 504.
10. Azuta, K.; Tadanaga, K.; Minami, T. J Ceram Soc Jpn 1999, 107, 293.
11. Wirnsberger, G.; Yang, P. D.; Scott, B. J.; Chmelka, B. F.; Stucky, G. D. Spectrochim Acta A 2001, 57, 2049.
12. Matsuda, A.; Matsuno, Y.; Katayama, S.; Tsuno, M.; Tohge, N.; Minami, T. J Ceram Soc Jpn 1994, 102, 330.
13. Kajihara, K.; Nakanishi, K.; Tanaka, K.; Hirao, K.; Soga, N. J Am Ceram Soc 1998, 81, 2670.
14. Lai, Y. C.; Valint, P. ACS Polym Mat Sci Eng 2002, 72, 116.
15. Jethmalani, J. M.; Ford, W. T.; Beaucage, G. Langmuir 1997, 13, 3338.
16. Atik, M.; Luna, F. P.; Messaddeg, S. H.; Aegerter, M. A. J Sol Gel Sci Technol 1997, 8, 517.
17. Misra, M.; Guest, A.; Tilley, M. Surf Coating Int 1998, 12, 594.
18. Donescu, D. Mat Plast 2001, 38, 3.
19. Masci, L. La Chimica e l'Industria 1998, 80, 623.
20. Baudrion, F.; Perichaud, A.; Vacelet, E. Biofouling 2000, 14, 317.
21. Saihi, D.; El-Achari, A.; Vroman, I.; Perichaud, A. J Appl Polym Sci 2005, 98, 997.
22. Uricanu, V.; Donescu, D.; Banu, A. G.; Serban, S.; Olteanu, M.; Dudau, M. Mat Chem Phys 2004, 85, 120.
23. Uricanu, V.; Donescu, D.; Banu, A. G.; Serban, S.; Vasilescu, M.; Olteanu, M.; Dudau, M. J Sol Gel Sci Technol 2005, 34, 23.
24. Banu, A. G.; Donescu, D.; Serban, S. Chem Bull Analele Univ Timisoara 2001, 46, 181
25. Wilkes, G.; Brenann, A.; Huang, H. H.; Rodrigues, D.; Wang, B. In Polymer Based Molecular Composites; Schafer, D. W.; Mark, J. E., Eds.; Material Research Society: Pittsburg, 1990; p 15.
26. Hubert-Pfalzagraf, L. G. Appl Organomet Chem 1992, 6, 627.
27. Donescu, D.; Serban, S.; Stanciu, L.; Braileanu, A.; Zaharescu, M. J Sol Gel Sci Technol 2000, 19, 839.
28. Donescu, D.; Serban, S.; Gosa, K.; Petcu, C. Central Eur J Chem 2004, 3, 1.
29. http://las.perkinelmer.com/content/ApplicationNotes/APP_ThermalContentSemicrystalnPolymers.pdf.
30. Fujiwara, M.; Grubbs, R. H.; Baldeschwieler, J. D. J Colloid Interface Sci 1997, 185, 210.
31. Andreas Maus, PhD Thesis, Albert-Ludwig Universiteit, Freiburg, Germany, 2005.
32. Reiter, G. Langmuir 1993, 9, 1344.
33. Hao, X.; Fan, X.; Wang, Z.; Wang, M. Mater Lett 2001, 51, 245.
34. Deshpande, A. V.; Kumar, U. J Non-Cryst Solids 2002, 306, 149.
35. Hinckley, D.; Seybold, P. G.; Borris, D. P. Spectrochim Acta 1986, 42A, 747.